ISSN 1063-7834, Physics of the Solid State, 2015, Vol. 57, No. 10, pp. 2059–2065. © Pleiades Publishing, Ltd., 2015.
Original Russian Text © S.V. Bobylev, I.A. Ovid'ko, 2015, published in Fizika Tverdogo Tela, 2015, Vol. 57, No. 10, pp. 2005–2010.

MECHANICAL PROPERTIES, PHYSICS OF STRENGTH, AND PLASTICITY

Thickening of Deformation-Distorted High-Angle Grain Boundaries in Nanomaterials

S. V. Bobylev[a, b, c] and I. A. Ovid'ko[a, b, c, *]

[a] *Research Laboratory "Mechanics of New Nanomaterials," St. Petersburg State Polytechnic University, ul. Politekhnicheskaya 29, St. Petersburg, 195251 Russia*

[b] *Institute of Problems of Mechanical Engineering, Russian Academy of Sciences, Bolshoi pr. 61, St. Petersburg, 199178 Russia*

* *e-mail: ovidko@nano.ipme.ru*

[c] *St. Petersburg State University, Universitetskaya nab. 7–9, St. Petersburg, 199034 Russia*

Received April 27, 2015

Abstract—A theoretical model describing deformation-distorted (nonequilibrium) high-angle grain boundaries in nanocrystalline and ultrafine-grained materials has been proposed. Within this model, the dislocation structure of the distorted high-angle grain boundaries has been considered as a combination of the standard wall of grain-boundary dislocations and lattice dislocations (nonequilibrium dislocations) trapped from the adjacent grains. The energy characteristics of a system of grain-boundary defects have been calculated. It has been shown that the thickening of a grain boundary due to the coordinated motion of nonequilibrium dislocations is an energetically favorable and barrierless process. The dependences of the thickening on different parameters of the problem have been investigated. Typical values of the thickening are equal to 1.5–2.5 nm, which agrees with the available experimental data.

DOI: 10.1134/S1063783415100054

1. INTRODUCTION

Nanocrystalline and ultrafine-grained materials (hereinafter, nanomaterials) are functional and structural materials of new generation with unique mechanical, physical, and chemical properties (see, for example, [1–6]). Nanomaterials are the subject of intense research [1–11] because of their paramount importance for present and future high technologies. In particular, nanomaterials are characterized by excellent mechanical properties that favorably distinguish them from conventional coarse-grained polycrystals with the same chemical composition. Examples of these properties are high values of tensile yield stress, ultimate strength, and wear resistance, as well as the ability of some nanocrystalline metals and alloys to undergo superplastic deformation [1–6]. Consequently, the physics of plastic deformation of nanomaterials is the subject of intense research motivated by a high potential of their practical application and by the fundamental interest in specific mechanisms of plastic deformation at the nanoscale level.

The unique properties of nanomaterials are associated with the size effects and nanostructures, where grain boundaries play an important role in deformation processes. Owing to the small grain size, the grain boundaries occupy a significant volume fraction of the material and, hence, play a decisive role in the formation of mechanical properties. On the other hand, conventional intragranular deformation mechanisms associated with the motion of lattice dislocations are substantially suppressed when the grains have small sizes. As a consequence, the majority of the mechanisms of plastic deformation in nanomaterials are controlled by grain boundaries [1–6]. Therefore, investigation of structural features of grain boundaries and their transformations is extremely important for the understanding of the processes occurring in nanomaterials during their deformation.

In their recent experiments, Sauvage et al. [12] revealed an interesting feature: an increase in the thickness (to 2–3 nm) of deformation-distorted (nonequilibrium) grain boundaries in bulk ultrafine-grained metal materials produced under severe plastic deformation. Earlier [11], we proposed a theoretical model of migration of deformation-distorted (nonequilibrium) low-angle grain boundaries [11], where among other things it was shown that these boundaries should expand (increase in their thickness) even in the absence of an external mechanical stress. This fact is confirmed by experimental observations [12] of the thickened grain boundaries in bulk ultrafine-grained materials produced under severe plastic deformation. However, in the experiments performed in [12], the authors, as a rule, observed high-angle grain boundaries with an increased thickness, whereas our previous work [11] dealt only with low-angle grain boundaries. The main purpose of the present work is to develop a theoretical model that effectively explains

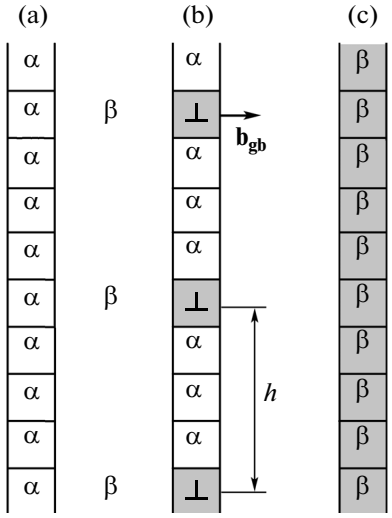

Fig. 1. Model of structural units of a high-angle grain boundary (schematically): (a) the grain boundary is formed only by structural units α, (b) the grain boundary consists of two types of structural units α and β (grain-boundary dislocations are bound to structural units β), and (c) the grain boundary is formed only by structural units β.

the thickening of deformation-distorted (nonequilibrium) high-angle grain boundaries in nanomaterials.

2. THICKENING OF DEFORMATION-DISTORTED HIGH-ANGLE GRAIN BOUNDARIES: GEOMETRICAL ASPECTS

For the description of the thickening of deformation-distorted (nonequilibrium) high-angle grain boundaries in nanomaterials, we generalize the model proposed in [11] to the case of high-angle grain boundaries. Within the approach used in [11], the nonequilibrium low-angle grain boundary was described as a combination of "equilibrium" and "nonequilibrium" dislocation ensembles. The first ensemble represents a conventional dislocation wall (or a symmetric tilt boundary), while the second ensemble is formed by lattice dislocations trapped by a grain boundary during the plastic deformation and randomly distributed along the boundary plane. A similar description can also be proposed for the case of high-angle grain boundaries. For this purpose, we use the model of structural units [13] for a conventional (equilibrium) high-angle grain boundary. In this model, the grain boundary is formed by periodically ordered structural units (atomic clusters) of two types (denoted as α and β, see Fig. 1). If, for example, the number of structural units β is smaller than that of structural units α, then the structural units β are referred to as minority structural units and described as cores of periodically distributed grain-boundary dislocations (Fig. 1b). These dislocations are characterized by the Burgers vectors $\mathbf{b}_{gb}$ (related to the translational symmetry of the grain boundary), whose modulus b_{gb} is usually less than the modulus of the Burgers vector **b** of lattice dislocations and lies in the range of $b/4$–$b/3$ [13]. In the case where the structural units β (or α) are completely absent (Figs. 1a, 1c), the misorientation angle of the boundary θ_α (θ_β) is determined exclusively by the geometry of the structural unit α (β), and the boundary is referred to as the preferred boundary. This boundary corresponds to a local energy minimum in the dependence of the grain-boundary energy on the misorientation angle. However, in the general case, the equilibrium high-angle grain boundary consists of structural units of two types (Fig. 1b), and the misorientation angle of this boundary is defined as $\theta = \theta_\alpha + \Delta\theta_\beta$, where $\Delta\theta_\beta$ is the contribution from the grain-boundary dislocations (structural units β) to the total misorientation of the boundary [13]. The angle $\Delta\theta_\beta$ is related to the period h of grain-boundary dislocations and the magnitude of their Burgers vector b_{gb} by the following expression:

$$\Delta\theta_\beta = 2\arctan(b_{gb}/2h). \quad (1)$$

Now, we use the above model as the basis for the model of a deformation-distorted high-angle grain boundary in a nanocrystalline material (Fig. 2). We consider the grain boundary *AB* of length *d* in a fragment of the nanocrystalline structure (Fig. 2a). Let this boundary be formed by structural units of two types; i.e., in accordance with the foregoing, it contains a periodic wall of grain-boundary dislocations characterized by the Burgers vector $\mathbf{b}_{gb}$. Next, according to the model of a low-angle grain boundary [11], we assume that the deformation-distorted high-angle grain boundary also contains nonequilibrium lattice dislocations of opposite signs ±**b** (Fig. 2b), which are trapped from the adjacent grains and randomly distributed along the boundary plane. As in the model developed in [11], we assume that the number of positive nonequilibrium dislocations is equal to the number of negative nonequilibrium dislocations, so that these dislocations do not affect the average misorientation of the grain boundary, thus providing only its local fluctuations around the average value of the misorientation angle θ.

The other grain boundaries (GB1–GB4) adjacent to the triple junctions *A* and *B* are assumed to be symmetric tilt boundaries. However, for simplicity, we will not consider their dislocation structure and, in order to take account of their influence on the migration of the boundary *AB*, we will use the disclination model [14]. According this model, the symmetric tilt boundary broken at one end can be approximately represented as a wedge disclination with the power equal to the misorientation angle of the grain boundary. If it is assumed that, initially, the junctions *A* and *B* are fully compensated (i.e., the sum of the misorientation angles of the grain boundaries meeting at this junction is zero), the misorientation angle θ of the boundary *AB* is equal to the sum of the misorientation angles of the

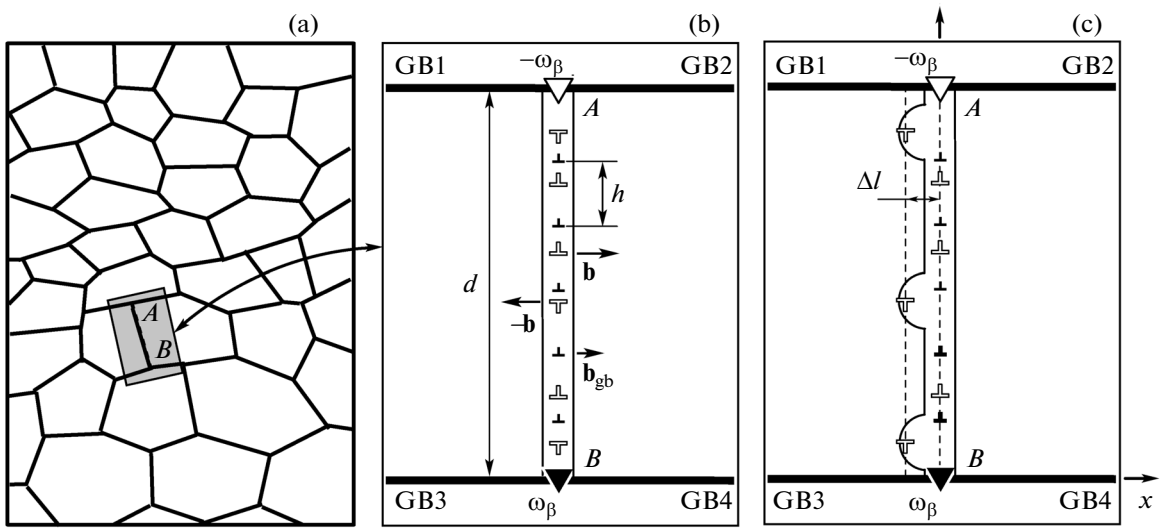

Fig. 2. Model of thickening of a deformation-distorted high-angle grain boundary with randomly distributed nonequilibrium dislocations. (a) Fragment of the nanocrystalline sample (general view). (b) Initial state. The nonequilibrium grain boundary *AB* is simulated as a combination of the wall of grain-boundary dislocations (indicated by dark symbols) and the "nonequilibrium" structure of the positive and negative lattice dislocations (indicated by open symbols). The influence of the adjacent grain boundaries (GB1–GB4) is described by the disclination dipole *AB* (for details, see the text). (c) Extended configuration of the grain boundary in which negative nonequilibrium dislocations are synchronously displaced by a distance Δl from the initial position.

other two boundaries with the opposite sign. Thus, in the equivalent disclination representation, the influence of the boundaries GB1–GB4 is considered as a dipole of wedge disclinations with the powers $\pm\omega_0$, where $\omega_0 = \theta$. Since the misorientation angle θ of the boundary *AB* consists of two parts determined by the structural units α and β ($\theta = \theta_\alpha + \Delta\theta_\beta$), the disclination dipole can be similarly represented as the sum of two dipoles: $\omega_0 = \omega_\alpha + \omega_\beta$, where $\omega_\alpha = \theta_\alpha$ and $\omega_\beta = \Delta\theta_\beta$. In the framework of our model, however, a part of the boundary *AB* represented by the structural units α is completely static and does not change during the transformation, which will be described below. The stress field of the structure α fully compensates for the stress field of the dipole ω_α, so that other defects (grain-boundary and nonequilibrium dislocations) do not interact with it. Consequently, in the calculation of the interaction with the boundaries GB1–GB4, it is sufficient to take into account the contribution $\omega_\beta = \Delta\theta_\beta$; i.e., the elastic stress fields induced by these boundaries are simulated by the dipole of wedge disclinations located in the junctions *A* and *B* and are characterized by the power $\pm\omega_\beta$ (Fig. 2b).

3. THICKENING OF DEFORMATION-DISTORTED HIGH-ANGLE GRAIN BOUNDARIES: ENERGY CHARACTERISTICS

The theoretical analysis performed in [11] demonstrated that, in nonequilibrium low-angle grain boundaries even in the absence of applied stresses, the energetically more favorable is a thickened configuration of the boundary, where negative nonequilibrium dislocations are collectively displaced from the initial plane of the boundary, as is shown in Fig. 2c. Further, it is demonstrated that, in the case of a high-angle grain boundary, the thickened configuration in Fig. 2c is also energetically more favorable than the initial configuration of the boundary (Fig. 2b). As in [11], we assume that the nonequilibrium dislocations are synchronously displaced in the form of a flat wall, and their positions can be described by a single parameter Δl, which characterizes the thickening of the high-angle grain boundary (Fig. 2c).

For this purpose, we write the change in the total energy of the system ΔW as a result of such process. It can be seen from Fig. 2c that the described transformation is accompanied by changes in the energy of interaction of negative nonequilibrium dislocations with the disclination dipole *AB* and all other dislocations (grain-boundary and positive nonequilibrium dislocations which remain in the initial positions). Hence, it follows that the quantity ΔW can be written as

$$\Delta W = \sum_{i=1}^{n/2}\sum_{j=1}^{k} W^{d-d}(-b, b_{gb}, \Delta l, y_j^{(gb)} - y_i^{(-)}) + \sum_{i=1}^{n/2}\sum_{j=1}^{n/2} W^{d-d}(-b, b, \Delta l, y_j^{(+)} - y_i^{(-)}) + \sum_{i=1}^{n/2} W^{\Delta-d}(-b, \Delta l, y_i^{(-)}) \quad (2)$$

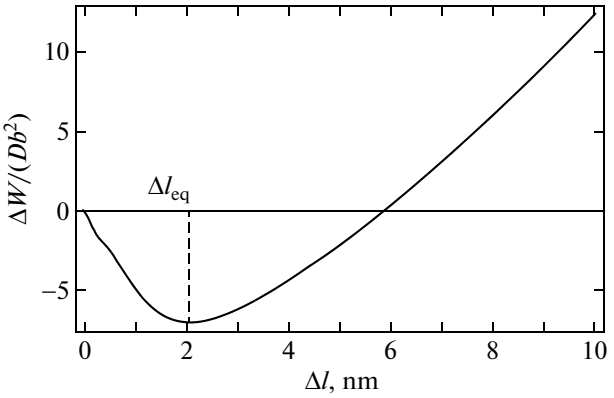

Fig. 3. Dependence of the change in the energy ΔW on the displacement Δl of negative nonequilibrium dislocations (grain-boundary thickenings) according to the calculation using aluminum as an example for the following parameters of the problem: $b_{gb} = b/3$, $h = 10b_{gb}$, and $d = 40$ nm.

$$-\sum_{i=1}^{n/2}\sum_{j=1}^{k} W^{d-d}(-b, b_{gb}, 0, y_j^{(gb)} - y_i^{(-)})$$
$$-\sum_{i=1}^{n/2}\sum_{j=1}^{n/2} W^{d-d}(-b, b, 0, y_j^{(+)} - y_i^{(-)})$$
$$-\sum_{i=1}^{n/2} W^{\Delta-d}(-b, 0, y_i^{(-)}).$$

Here, $W^{d-d}(b_1, b_2, x_i - x_j, y_i - y_j)$ is the energy of interaction between two edge dislocations (with the parallel Burgers vectors $\mathbf{b}_1$ and $\mathbf{b}_2$) located at the points with the coordinates $(x_i, y_{i)}$ and (x_j, y_j), respectively (hereinafter, we use the coordinate system presented in Fig. 2c); $W^{\Delta-d}(b, x_i, y_i)$ is the energy of interaction between the disclination dipole and the dislocation with the Burgers vector $\mathbf{b}$ (perpendicular to the axis of the dipole), which is located at the point with the coordinates (x_i, y_i); n is the number of nonequilibrium dislocations (it is an even number, because the numbers of positive and negative nonequilibrium dislocations are assumed to be identical); k is the number of grain-boundary dislocations; $y_i^{(gb)} = ih$ is the y-coordinate of the ith grain-boundary dislocation ($i = 1, 2, ..., k$); and $y_i^{(+)}$ and $y_i^{(-)}$ are the y-coordinates of the positive and negative nonequilibrium dislocations, respectively ($i = 1, 2, ..., n/2$). The numbering of dislocations in formula (2) goes from the junction B (Fig. 2) and is separate for the grain-boundary, positive, and negative nonequilibrium dislocations. Taking into account that the grain-boundary dislocations are distributed periodically (with the period h), from the elementary geometrical considerations their number k is expressed as follows:

$$k = [d/h]. \quad (3)$$

Here, the notation $[x]$ means the integer part of x. The number of nonequilibrium dislocations n in the framework of our model is set arbitrarily.

The energies $W^{d-d}(b_1, b_2, x_i - x_j, y_i - y_j)$ and $W^{\Delta-d}(b, x_i, y_i)$ are well known (see, for example, [14, 15]) and have the form

$$W^{d-d}(b_1, b_2, x_i - x_j, y_i - y_j) = Db_1b_2$$
$$\times\left(\ln\frac{R}{\sqrt{(x_i - x_j)^2 + (y_i - y_j)^2}} - \frac{(y_i - y_j)^2}{(x_i - x_j)^2 + (y_i - y_j)^2}\right), \quad (4)$$

$$W^{\Delta-d}(b, x_i, y_i) = D\omega_\beta b$$
$$\times\left[(y_i - d)\ln\frac{R}{\sqrt{x_i^2 + (y_i - d)^2}} - y_i\ln\frac{R}{\sqrt{x_i^2 + y_i^2}}\right], \quad (5)$$

where $D = G/[2\pi(1 - \nu)]$, G is the shear modulus, ν is the Poisson's ratio, and R is the screening radius of elastic stresses of the dislocation and disclination defects. Taking into account formula (1) and the fact that the power is $\omega_\beta = \Delta\theta_\beta$, the power of a disclination dipole can be expressed through the period of the grain-boundary dislocation wall h and the magnitude of the Burgers vector b_{gb} in the form $\omega_\beta = 2\arctan(b_{gb}/2h)$.

Thus, we found all the necessary (expressions (2)–(5)) for calculating the change in the energy ΔW. The final expression is not given here because of its bulkiness.

Next, we calculated the energy ΔW for aluminum used as an example. This material is characterized by the following parameters [15]: $G = 73$ GPa, $\nu = 0.34$, and $b = 0.25$ nm. Figure 3 shows the characteristic dependence $\Delta W(\Delta l)$ calculated for the parameters of the problem $b_{gb} = b/3$, $h = 10b_{gb}$, and $d = 40$ nm. (Formulas (4) and (5) also include the screening radius R, but, using expression (2), we can demonstrate that the change in the energy ΔW does not depend on R.) For definiteness, the nonequilibrium dislocations in this case are distributed periodically as follows: $y_i^{(+)} = b + 2(i - 1)p$ and $y_i^{(-)} = b + 2ip$ ($i = 1, 2, ..., n/2$), where $p = 5b$ is the repetition period of nonequilibrium dislocations. For this definition of the coordinates of dislocations, their number n is specified as $n = [(d - 2b)/p]$ (in the case where this number is odd, it is decrease by unity); for the parameters given above, the curve shown in Fig. 3 corresponds to $n = 26$. The curve $\Delta W(\Delta l)$ shown in Fig. 3, according to our analysis, is absolutely typical for any (not only periodic) distribution of nonequilibrium dislocations. There is always a minimum of the change in the energy for an equilibrium value of $\Delta l_{eq} > 0$; i.e., the initial state of the boundary (Fig. 2b) is not stable. In this case, the tran-

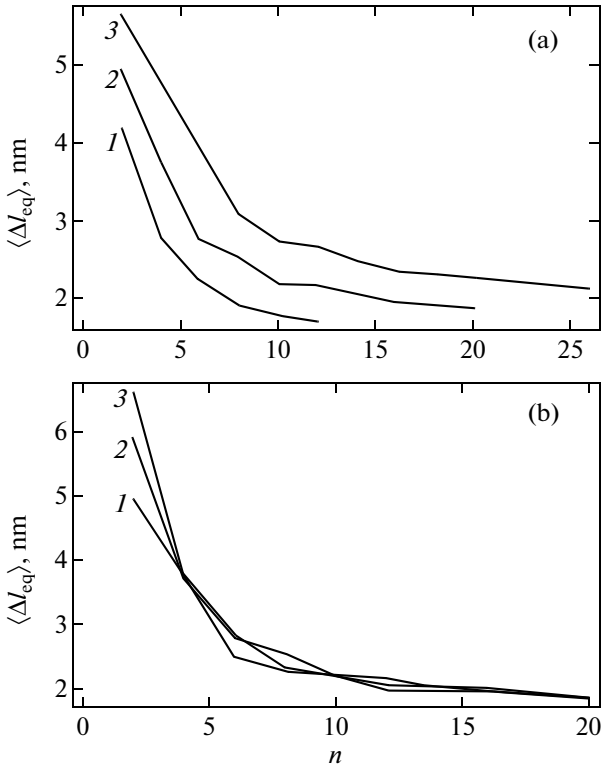

Fig. 4. Calculated dependences of the average grain-boundary thickening $\langle \Delta l_{eq} \rangle$ in aluminum on the number of nonequilibrium dislocations n: (a) $h = 10b_{gb}$ and $d =$ (*1*) 20, (*2*) 30, and (*3*) 40 nm; (*b*) $d = 30$ nm and $h =$ (*1*) $10b_{gb}$, (*2*) $15b_{gb}$, and (*3*) $20b_{gb}$.

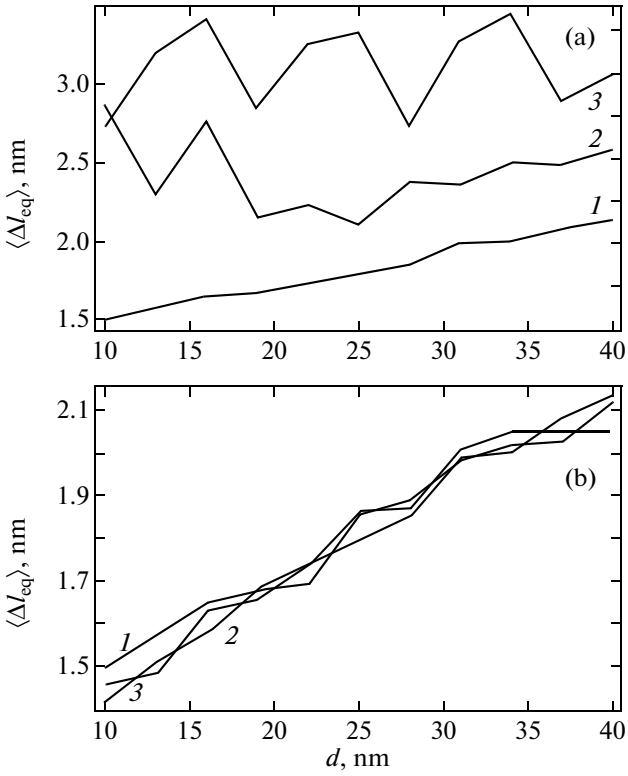

Fig. 5. Calculated dependences of the average grain-boundary thickening $\langle \Delta l_{eq} \rangle$ in aluminum on the grain size d of nonequilibrium dislocations. (a) $h = 10b_{gb}$ and $\langle p \rangle =$ (*1*) $5b$, (*2*) $10b$, and (*3*) $15b$; (b) $\langle p \rangle = 5b$ and $h =$ (*1*) $10b_{gb}$, (*2*) $15b_{gb}$, and (*3*) $20b_{gb}$.

sition to the stable state from the initial configuration (Fig. 2b) is a barrierless process and should occur spontaneously; i.e., nonequilibrium high-angle grain boundaries have a tendency to thickening.

Further, we investigated the dependence of the thickening Δl_{eq} on different parameters of the problem (also for aluminum used as an example), namely, the number of nonequilibrium dislocations n (Fig. 4), the length of the grain boundary d (Fig. 5), and the period of the structure of grain-boundary dislocations h (Fig. 6). In this analysis, we considered random distributions of nonequilibrium dislocations and used the following calculation scheme. For a given set of parameters of the problem, 1000 random distributions of nonequilibrium dislocations were generated and, for each distribution, the equilibrium thickening Δl_{eq} was determined. Then, the equilibrium thickening Δl_{eq} was averaged over all the generated distributions, and the average value of the thickening $\langle \Delta l_{eq} \rangle$ was determined.

Figure 4a shows the dependences $\langle \Delta l_{eq} \rangle(n)$ calculated for the parameters $h = 10b_{gb}$ and $d = 20$, 30, and 40 nm (curves *1–3*, respectively). The dependences $\langle \Delta l_{eq} \rangle(n)$ shown in Fig. 4b are calculated for the parameters $d = 30$ nm and $h = 10b_{gb}$, $15b_{gb}$, and $20b_{gb}$ (curves *1–3*, respectively). The other parameters of the problem are the same as in the previous case. The maximum value of n, which was used in constructing the curves shown in Fig. 4, corresponds to the average distance between the nonequilibrium dislocations $\langle p \rangle \sim 5b$. It can be seen from Fig. 4 that the typical values of $\langle \Delta l_{eq} \rangle$ lie in the range from 1.5 to 5 nm. Moreover, the average thickening $\langle \Delta l_{eq} \rangle$ is larger for the grain boundaries with a smaller number of nonequilibrium dislocations; i.e., the larger is the number of nonequilibrium dislocations in the grain boundary, the more resistant is the boundary to thickening. It should be, however, kept in mind that, for a very small number of nonequilibrium dislocations (for example, for $n = 2$, there is only one negative nonequilibrium dislocation), we cannot consider the thickening of the grain boundary as a whole; rather, we are dealing here with the emission of a single dislocation from the grain boundary. The grain boundaries with a sufficiently high density of nonequilibrium dislocations are characterized by the values $\langle \Delta l_{eq} \rangle \sim 1.5–2.5$ nm. These values correlate well with the experimentally observed [12] boundaries of approximately the same thickness in bulk ultrafine-grained materials.

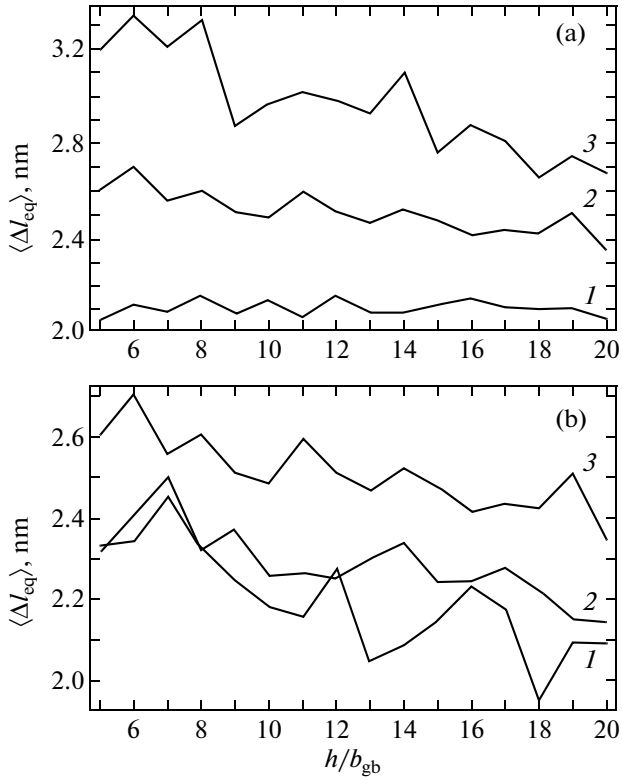

Fig. 6. Calculated dependences of the average grain-boundary thickening $\langle \Delta l_{eq} \rangle$ in aluminum on the period h of the grain-boundary dislocation structure: (a) $d = 40$ nm and $\langle p \rangle = (1)\ 5b$, $(2)\ 10b$, and $(3)\ 15b$; (b) $\langle p \rangle = 10b$ and $d = (1)\ 20$, $(2)\ 30$, and $(3)\ 40$ nm.

The dependences $\langle \Delta l_{eq} \rangle(d)$ are illustrated in Fig. 5. The curves shown in Fig. 5a are calculated for the parameters $h = 10b_{gb}$ and $\langle p \rangle = 5b$, $10b$, and $15b$ (curves *1–3*, respectively). Figure 5b shows the curves calculated for the parameters $\langle p \rangle = 5b$ and $h = 10b_{gb}$, $15b_{gb}$, and $20b_{gb}$ (curves *1–3*, respectively). The number of nonequilibrium dislocations is related to the average distance $\langle p \rangle$ between them as follows: $n = [(d - 2b)/\langle p \rangle]$. It is clearly seen that there is a tendency to an increase in the average thickening $\langle \Delta l_{eq} \rangle$ with increasing grain size. The curves corresponding to low densities of nonequilibrium dislocations (large values of $\langle p \rangle$) have significant oscillations due to the discrete character of the model and the errors of the averaging.

The dependences $\langle \Delta l_{eq} \rangle(h)$ are presented in Fig. 6. The curves shown in Fig. 6a are calculated for the parameters $d = 40$ nm and $\langle p \rangle = 5b$, $10b$, and $15b$ (curves *1–3*, respectively). Figure 6b shows the curves calculated for the parameters $\langle p \rangle = 10b$ and $d = 20$, 30, and 40 nm (curves *1–3*, respectively). It can be seen that the thickening weakly depends on the period of the grain-boundary dislocation structure (actually, on the misorientation angle of the grain boundary) with a slight tendency to a decrease in the average thickening $\langle \Delta l_{eq} \rangle$ with increasing period h.

4. CONCLUSIONS

Thus, in this work, we proposed a theoretical model that effectively describes a deformation-distorted high-angle grain boundary on the basis of the model proposed in our recent work [11] for deformation-distorted of low-angle grain boundaries and the model of structural units [13], which describes conventional (deformation-undistorted) high-angle grain boundaries. Within this model, the structure of a grain boundary is described as a combination of the standard periodic wall of grain-boundary dislocations and a random distribution of nonequilibrium lattice dislocations of opposite signs that are trapped from the adjacent grains (Fig. 2). It was shown that the extended configuration (Fig. 2c), in which negative nonequilibrium dislocations are displaced with respect to the boundary plane by some distance Δl_{eq}, is energetically more favorable than the configuration where all dislocations are in the same plane (Fig. 2b). The transition between these two states is a barrierless process and occurs spontaneously even in the absence of external stresses. We investigated the dependences of the averaged thickening $\langle \Delta l_{eq} \rangle$ for a set of random distributions of nonequilibrium dislocations on the number of nonequilibrium dislocations, grain size (the grain-boundary length), and the period of the structure of grain-boundary dislocations. It was demonstrated that typical values of $\langle \Delta l_{eq} \rangle$ lie in the range of ~1.5–2.5 nm, which correlates well with the experimentally observed [12] boundaries of approximately the same width in bulk ultrafine-grained materials.

ACKNOWLEDGMENTS

This study was supported by the Russian Science Foundation (project no. 14-29-00199).

REFERENCES

1. I. A. Ovid'ko, Int. Mater. Rev. **50**, 65 (2005).
2. M. Dao, L. Lu, R. J. Asaro, J. T. M. De Hosson, and E. Ma, Acta Mater. **55**, 4041 (2007).
3. C. S. Pande and K. P. Cooper, Prog. Mater. Sci. **54**, 689 (2009).
4. C. C. Koch, I. A. Ovid'ko, S. Seal, and S. Veprek, *Structural Nanocrystalline Materials: Fundamentals and Applications* (Cambridge University Press, Cambridge, 2007).
5. Y. Estrin and A. Vinogradov, Acta Mater. **61**, 782 (2013).
6. G. A. Malygin, Phys.—Usp. **54** (11), 1091 (2011).
7. R. F. Al'mukhametov, L. A. Gabdrakhmanova, I. Z. Sharipov, and Ya. F. Abzgil'din, Phys. Solid State **56** (2), 223 (2014).

8. O. A. Maslova, F. V. Shirokov, Yu. I. Yuzyuk, M. E. Marssi, M. Jain, N. Ortega, and R. S. Katiyar, Phys. Solid State **56** (2), 310 (2014).

9. N. V. Tokiy, V. V. Tokiy, A. N. Pilipenko, and N. E. Pis'menova, Phys. Solid State **56** (5), 1002 (2014).

10. V. A. Moskalenko, V. I. Betekhtin, B. K. Kardashev, A. G. Kadomtsev, A. R. Smirnov, R. V. Smolyanets, and M. V. Narykova, Phys. Solid State **56** (8), 1590 (2014).

11. S. V. Bobylev and I. A. Ovid'ko, Acta Mater. **88**, 260 (2015).

12. X. Sauvage, G. Wilde, S. V. Divinski, Z. Horita, and R. Z. Valiev, Mater. Sci. Eng., A **540**, 1 (2012).

13. A. P. Sutton and R. W. Balluffi, *Interfaces in Crystalline Materials* (Oxford University Press, Oxford (1996). .

14. V. I. Vladimirov and A. E. Romanov, *Disclinations in Crystals* (Nauka, Leningrad, 1986) [in Russian].

15. J. P. Hirth and J. Lothe, *Theory of Dislocations* (Wiley, New York, 1982).

Translated by O. Borovik-Romanova